An individual based model with global competition interaction: fluctuations effects in pattern formation

E. Brigatti $^{\star\pm}$, V. Schwämmle† and Minos A. Neto*

$\dagger$*Centro Brasileiro de Pesquisas Físicas, Rua Dr. Xavier Sigaud 150, 22290-180, Rio de Janeiro, RJ, Brazil*
$\star$*Instituto de Física, Universidade Federal Fluminense, Campus da Praia Vermelha, 24210-340, Niterói, RJ, Brazil*
$\pm$*e-mail address: edgardo@if.uff.br*
(September 16, 2013)

We present some numerical results obtained from a simple individual based model that describes clustering of organisms caused by competition. Our aim is to show how, even when a deterministic description developed for continuum models predicts no pattern formation, an individual based model displays well defined patterns, as a consequence of fluctuations effects caused by the discrete nature of the interacting agents.

87.17.Aa,87.23.Kg, 87.23.-n, 05.10.Ln

I. INTRODUCTION

Spatial patterns due to clustering of organisms can be generated by some kind of frequency-dependent interaction, that represents competition between individuals. This feature has attracted the interest of a variety of fields ranging from pure mathematics [1] and non-linear physics [2–6] to population biology [7,8] and theoretical studies in evolutionary theory [9]. A striking fact related to this phenomenon is the appearance of a transition (*segregation transition* [2]), for specific values of the parameters and for some forms of the interaction. This transition drives the steady state of the system from a spatially homogeneous distribution to one characterized by some clearly distinguishable inhomogeneities.

Here we consider models that take into account diffusion effects and a direct implementation of birth and death processes, making them ideal to describe biological processes.

These models permit multiple interpretations. In a common interpretation the system space directly represents the physical space where the organisms live and the diffusion represents their spatial movement. Competition between individuals corresponds to a mechanism of growth control caused by limited common resources. In this case, pattern formation can reproduce the evolution of bacterial colonies, plankton concentration [10], development of vegetation or spatial distribution of predators.

On the other hand, a different interpretation enables us to describe the speciation process: the generation of two different species starting from one single continuous population of interbreeding organisms. To be specific, we can describe the speciation process by representing all the phenotypic characteristics that determine the biological success of an individual by a number, the strategy value, that labels each individual. By reproduction, that includes a mutation process, an offspring inherits a strategy that slightly differs from the one of its parent. In order to model natural selection, a frequency-dependent

mechanism that mimics competition, completes the ingredients necessary for the emergence of population clustering. In this scenario, the generation of a new cluster is interpreted, in a broad sense, as a speciation event [9]. Now, if the model space represents the mentioned strategy space and the diffusion models the mutation process during reproduction, we can identify the mechanism of growth control with natural selection and the branching events with the speciation process. This different interpretation justifies the analogy between a model that describes the speciation process and the ones that describe spatial pattern formation in the evolution of bacterial colonies, vegetation or predation.

We can describe such processes starting from an individual based model, that yields information on the behavior of a finite system (finite population) and accounts for fluctuation effects caused by the discrete nature of the interacting agents. Another approach starts from a continuous mean-field description, that is exact in the infinite-size limit but neglects fluctuations.

Choosing this second strategy, the generalization of a well-investigated equation (Fisher-Kolmogoroff-Petrovsky-Piscounoff [11]) is quite common at present. In addition to a diffusion process with coefficient D and a population growth mechanism (rate a), this equation incorporates a growth-limiting process controlled by the parameter b [3,4,6]:

$$\frac{\partial \rho(x,t)}{\partial t} = D\nabla^2 \rho(x,t) + a\rho(x,t) - \qquad (1.1)$$

$$b\,\rho(x,t) \int_{-\infty}^{+\infty} \rho(y,t)F(x,y)dy \ ,$$

where ρ is the density of individuals at position x and time t. Competition is obtained by varying the death probability for each individual, and is controlled through the *influence function* $F(x,y)$. Let us focus on the shape of the influence function: it can range from a simple box-like function to a global uniform interaction. However,

1

the Gaussian function should be considered particularly relevant. If, for instance, we need to represent the activity of a sedentary animal the interaction represented in the influential function should take into account the individual's daily excursion around the fixed breeding site that can be represented by Brownian motion and, for this reason, by a Gaussian distribution. In the same way, if we want to represent the habitat degeneration induced by the growing of a colony of plants we can think that the colony is originated by a single individual that disperses its seeds in a way also well described by Brownian motion. More generally, for a biological interaction that does not stop at some defined length (presence of a cutoff), and that is nonlocal and controlled by a pure stochastic process, the Gaussian function should be the most natural choice. On the other hand, this choice is a source of complications.

Deterministic descriptions, in the case of a Gaussian influence function, predict no pattern formation [4,12]. However, such descriptions do not take into account fluctuations arising from the discrete character of individuals. The importance of these fluctuations have been recently pointed out in a quite paradigmatic example, where random walking organisms that reproduce and die at a constant rate spontaneously aggregate [10,13]. The deterministic approximation is not able to show this behavior, incapable of capturing the essential asymmetry between birth, a multiplicative process that increments the density in the regions adjacent to the parent, and death events, that occur anywhere. Even when the patterns can be obtained within the deterministic description, a recent work outlines the importance of fluctuations by showing their impact on affecting transition points and amplitudes [6,14,15].

In this work we present some numerical results obtained by means of a simple individual based model. Our aim is to show the appearance of a *segregation transition* in a model where the deterministic instability, produced by the non-local interaction, is not sufficient for generating inhomogeneities [4], but the superimposed microscopic stochastic fluctuations permit the emergence of patterns. Moreover, we want to characterize the behavior of such a model by analyzing finite size effects, general conditions that allow spatial segregation of arbitrary wavelengths, cluster size dependence on diffusion rate and population size, fluctuations. Finally, we compare the model implementation in the strategy space with the implementation in the physical space. In the first, used to characterize the speciation process, diffusion amounts to a mutation phenomenon, operating just one time in each individual's life. In the second, directly related to the reaction-diffusion equation (eq. (1.1)), diffusion describes a typical Brownian motion.

II. THE MODEL

The simulations start with an initial population of N_0 individuals located along a ring of length L. At each time step, our model is controlled by the following microscopic rules:

1) Each individual, characterized by its position x, dies with probability P,

$$P = K \cdot \sum_{j=1}^{N(\tau)} \exp(-\frac{(x - y_j)^2}{2C^2}) , \qquad (2.1)$$

where $N(\tau)$ is the total number of individuals at the actual step τ and y_j is the respective individuals' positions. The strength of competition declines with distance according to a Gaussian function with deviation C. The parameter K depicts the carrying capacity.

2) If the individual survives this death selection, it reproduces. The newborn, starting from the parent's location, moves in random direction a distance obtained from a Gaussian distribution of standard deviation σ. This change represents the effect of mutations in the offspring phenotype.

As soon as all the individuals passed the death selection and eventually reproduced, the next time step begins. This model implementation is analogous to the diffusion process described by eq. (1.1). To establish a direct comparison between that mean field description and the individual based simulation we have also implemented the model with an exact microscopic representation of the diffusion term. In this case, changing the second step of our algorithm, the rules become:

1) Each individual with strategy x dies with the probability obtained from eq. (2.1).

2) If the individual survives the death selection it reproduces and the newborn maintains the same location of the parent.

3) After reproduction, Brownian motion lets the individual move a distance, in random direction, chosen from a Gaussian distribution of standard deviation σ.

If, in eq. (1.1), we measure time in units of the simulation time step, the coefficient D is related to our simulation parameter through $D \propto \sigma^2$. The influence function is given by a Gaussian of standard deviation C and the growth rate is $a = 1 - P$, with P given by eq. (2.1).

Essentially, the only difference between these two versions of our model is that in the first one individuals move only at birth, while in the second version they move at every time step along their life. Since the death probability, at equilibrium, is approximately $1/2$, usually, even in the second version, an individual moves just one time during its life. For this reason, there are no sensitive differences between the two model implementations, as shown by the measures reported in section IV.

III. MODULATION

In the following we present some typical examples of steady states generated by the dynamics of the model.

For a global competition that results to be extremely long-ranged (large C values, in relation with the values of parameters σ and K), the steady state is characterized by a spatially homogenous occupancy. If the σ value is sufficiently large or/and the K value sufficiently small, totally homogeneous distributions are obtained (Figure 1), otherwise the solution is smooth but with the population concentrated in one region of the ring, with its width controlled by σ.

As stated above, a simple heuristic analysis of eq. (1.1) in the Fourier space shows that there is a necessary condition for the emergence of inhomogeneity: the Fourier transform of the influence function must have negative values and large enough magnitude [4,5]. A Gaussian in an infinite domain has a positive counterpart in Fourier space and so does not match such requirements. In contrast with these results, the fluctuations present in the discrete model arrive to excite one specific mode [14] and modulations of this wavelength appear. The tuning of the parameters allows modulations of arbitrary wavelengths (Figure 1).

When C is decreased, the competition between modes becomes stronger and no single mode dominates. In this situation, some small regions of the ring are occupied forcing all the remaining areas, up to some range, to be nearly empty. The landscape results populated by several living colonies divided by dead regions. There is almost no competition between individuals of different colonies and the space separating them can be identified with an effective interaction length. This steady state (*spiky state* [2]) corresponds to a sequence of isolated colonies (spikes) and seen in the Fourier space, many active wavelengths contribute to it (Figure 2).

Finally, for extreme short-ranged competition, in relation to the σ value, no collective cooperation between different excited modes emerges and a noisy spatially homogeneous distribution appears (Figure 2).

We describe these paradigmatic steady states of the system by characterizing the related spatial structure with the help of a *structure function* $S(q)$ [6] defined as follows:

$$S(q) = \left\langle \left| \frac{1}{N(t)} \sum_{j=1}^{N(t)} \exp[i2\pi q \cdot x_j(\tau)] \right|^2 \right\rangle_T \qquad (3.1)$$

where the sum is performed over all individuals j with their positions determined by $x_j(\tau)$. The function is averaged over some time interval T in order to avoid noisy data. The maxima of this function identify the relevant periodicity present in the steady state. $S(0)$ corresponds to the square of the mean number of individuals in the system. We will see that the position of the global maximum (q_M) provides an appropriate order parameter for the identification of the segregation transition.

In our study we explored two different initial conditions. In the first (local i.c.), the colony is located in a finite and compact region of the space. In the second (global i.c.), the individuals are spread all over the space. The final distribution is independent of this choice and, generally, local initial conditions make the system reach the steady state slower. For this reason, if not differently specified, our results are obtained from global initial conditions.

IV. FINITE SIZE EFFECTS

Our analysis starts by exploring the model dependence on the space size L. We test if the pattern formation is not merely a product of some finite size effect. This is important, in the light of what was reported by Fuentes *et al.* in ref. [4]. In their work, a numerical solution of eq. (1.1) with a Gaussian influence function, showed a segregation transition. But such a transition was just the effect of the finite domain size that acted like a cut-off for the Gaussian. Evidence of this interpretation came from the observation that the amplitude of the patterns depended on the ratio of the standard deviation of the influence function to the domain size - the critical values of the standard deviation corresponding to the segregation transition depended linearly on the domain size - and the same patterns appeared for a modified Gaussian, which vanishes abruptly beyond a cutoff. The study of our individual based model gave different results. Running some simulations with exactly the same parameters but changing the ring extension, we were able to show that the system is not influenced by the domain size. If we choose data from spiky steady states, that permit clear quantitative measures, it is possible to remark that the general morphology of the patterns do not change increasing the L value. In fact, the population density and the mean number of peaks remains constant (they linearly scale with L). Moreover, in order to provide a more precise test of possible little variations in the distribution, we measured the cluster size. This quantity was calculated by evaluating the standard deviation $(< x^2 >_i - < x >_i^2)^{1/2}$ of the position of the i individuals confined in each peak, than averaged over the different peaks present at step τ and, finally, averaged over many time steps after the system has reached the steady state.

Varying the system size caused no changes in the clusters size (see Figure 3). From this result, we concluded that the general aspect of the steady state does not change with L. In particular, in contrast with what happens when the mean field equation is solved numerically, the patterns do not depend on the ratio $\frac{C}{L}$. For example,

for $C = 0.2$ and $L = 50$ we obtained a spiky steady state, for $C = 0.004$ and $L = 1$ (same ratio) we obtained an homogeneous steady state. Taking into account these results, from now on, all our simulations are implemented on a ring of size 1.

We have just shown how the average of the population size $<N>$ scales with L in the steady state. An estimation of $<N>$, as a function of the parameters K and C, can be obtained throw a simple heuristic argument. We can assume that, locally and in the steady state, the number of deaths must be, on average, compensated by the number of newborns, in order to comprise a stable population. For this reason, the death probability P must equal $1/2$. Assuming that the number of neighbors that compete with a single individual are the ones living up to a distance C and that, in this surrounding, the average density N/L can be considered to be uniform, P reduces to $K \cdot 2C \cdot N/L$. Thus, $N \propto L/(CK)$. Looking at Figure 4 we can see that this crude evaluation, that neglects diffusion, inhomogeneity and reduces the influence function to a box, describes well the general behavior of the data obtained from our simulations.

V. SEGREGATION TRANSITION

The structure function introduced in eq. (3.1) provides a proper order parameter to describe the segregation transition. Different regions in the parameter space, coinciding with different steady states, correspond to different positions of the global maximum of the structure function. The transition from an homogeneous to a inhomogeneous distribution (see Figure 2) matches the jump of the position of the global maximum (q_M) to a clear integer value, correspondent to the number of clusters present in the space. For this reason we can characterize the transition looking at the shape assumed by $S(q)$, or looking at the value of q_M. If the space is homogeneously occupied, the structure function does not present an integer maximum. On the contrary, the maximum is located at $q_M \simeq 1.4$. This value corresponds to an uniform distribution of individuals in the interval $[0,1]$, approximated by the expression $\left| \int_0^1 \exp(i2\pi q \cdot x)dx \right|^2$. The segregation transition is characterized by the passage of $S(q)$ from 1.4 to an integer value. In Figure 5 we show q_M as a function of C, varying K and σ. First of all, from the analysis of these data, we can observe that the number of clusters scales as C^{-1} (or, equivalently, the periodicity of the inhomogeneous phase has wave lengths proportional to C). Moreover, a critical value of C exists for which the transition takes place. This C_{critic} grows with $1/K$ and with σ. An analysis of the available data suggests the possible dependence: $C_{critic} \propto \sigma^{2/3}K^{-1/3}$. Finally, for larger values of the parameter C, in this range of the parameters σ and K, the distributions are characterized by just one peak.

For any value of the competition strength, as can be seen in Figure 6, there exists a critical value σ_{critic}, dependent on C and K, above which no spatial structures emerge. Another measurement, that permits to state this relation in a different and clearer way, is presented in the next paragraph.

VI. CLUSTER SIZE AND FLUCTUATIONS

We analyzed the typical size S of the clusters that appears in the spiky phase. The data exposed in Figure 7 show a dependence of the cluster size on the diffusion coefficient: $S \propto \sigma$, equivalent to $S \propto \sqrt{D}$. These results are in accordance with the data presented in ref. [15] obtained from an individual based model. In addition, this work pointed out how this behavior deviates from the conclusions obtained from the deterministic approximation, where the cluster size was only weakly dependent on the diffusion coefficient.

We can imagine that the individuals confined in a cluster diffuse a distance proportional to $\sqrt{DJ}$ where J is the number of jumps the individual performs in its life. In the case of the first implementation of the model, where the diffusion is due to the mutation process, J is obviously one. However, the same results are obtained also with the second implementation (see Figure 7), by the fact that the mean lifetime of each individual is one. Finally, we present S as a function of K: $S \propto \sqrt{1/K}$. The reasons for this behavior are already explained in ref. [16]: the cluster size is not controlled just by the single individual number of jumps, in fact the diffusive process continues with its descendants. For this reason, it is proportional to the mean lifetime of a family, estimated to be proportional to K^{-1} (see ref. [16] for details).

We introduced a new quantity, the *mobility $M(\tau)$*, to estimate the mean mobility of individuals. At a given time step τ, we choose an individual i. Then we look for the closest agent, among all the population, at time step $\tau - 1$. We identify with d_i the distance between these two individuals. Averaging over the entire population $N(\tau)$ we obtain:

$$M(\tau) = \frac{1}{N(\tau)} \sum_{i=1}^{N(\tau)} d_i. \tag{6.1}$$

The values assumed by M by varying the parameters σ and C are shown in Figure 8. It is easy to distinguish two clearly different behaviors. If the system is organized in a spiky state, $M(\tau) \propto \sigma$. M is another way of measuring the mean distance that an individual moves during its lifetime inside the region defined by the cluster. For this reason, this measure is coherent with the data obtained from the direct evaluation of the standard deviation of

the clusters. In contrast, when the system is organized in the homogeneous phase (when $\sigma > \sigma_{critic}$) M becomes independent of σ and is directly proportional to the occupation density $M(\tau) \propto KC$. For this reason, collapsing these data permits to obtain, in a different way, the dependence of σ_{critic}:

$$\sigma_{critic} \propto C\sqrt{K} \qquad (6.2)$$

We conclude our study with some measurements trying to catch some properties of the system fluctuations. First, we estimated the fluctuations of the total population, averaging over different simulations. It resulted that the variance is constant along the time evolution and of the order of the square root of the total population. The mechanism of auto-regulation of the population dimension (2.1) does not allow the growth of big differences in the total number of individuals.

For this reason, we focused our attention on the spatial distribution of the population and tried to measure some properties of these fluctuations. We studied the variation of the local number of individuals in the same simulation, for different times. We analyzed the evolution of the system starting from local initial conditions, with the population concentrated in the interval $[0.49, 0.51]$. In this situation, the system evolves in time with a little cluster fluctuating around the initial space interval. This situation changes when a branching event occurs that generates two well-defined clusters. Our interest is to show the behavior of local space fluctuations and capture possible variations in correspondence with the branching event. First of all, we looked at the mean value of the spatial local fluctuations $F_s(\tau)$, defined as $F_s(\tau) = (\sum_{j=1}^{b} f_j^2)^{1/2}$, where f_j is the occupancy variation of the bin j from time step $\tau - 1$ to time step τ. We performed the average over all the b bins the ring was divided in and obtained $F_s(\tau) = \sqrt{N(\tau)}$, with no relevant variations throughout the time evolution, even in the time interval correspondent to the branching event. More interesting is the shape of the frequency distribution of the size of f_j. In fact, a simple Gaussian does not fit this distribution, that presents extended tails (see Figure 9). Along the system time evolution, the shape of the normalized distribution is conserved. For global initial conditions the same frequency distribution, with extended tails, is recovered at the steady state. It is identical to the one obtained with local initial conditions and measured at the steady state. We think that the distribution deviation from a Gaussian can be considered as a hint that fluctuations play a relevant role in the dynamics of the systems.

VII. CONCLUSIONS

We presented some results regarding clustering of organisms caused by a frequency-dependent interaction that represents competition. We showed how this way of modeling competition can be used not only to describe spatial phenomena in population biology, but also, through a more abstract interpretation, to test ideas of evolutionary theory (for example, studying the speciation process).

From this unifying perspective, our study, obtained from an extensive collection of data coming from simulations of an individual based model with global competition, pointed out the relevance of fluctuations effects in pattern formation. For the influence function adopted, the mean field description predicts the absence of spatial structures. On the contrary, fluctuations are able to excite the emergence of well defined patterns, which can not be generated from a deterministic instability.

Furthermore, we discussed other fundamental properties of our model in the light of the existing literature, unfolding a comparison with other models that describe spatial segregation originated by some deterministic instability. We showed that the observed patterns are not due to a finite size effect, we characterized the behavior of the segregation transition in various regions of the parameter space and studied the existence of a critical diffusion value. We analyzed the dependence of the cluster size on the diffusion coefficient and pointed out some characteristics of the fluctuations of the system.

[1] N. F. Britton, SIAM J. Appl. Math. **50**, 1663 (1990), S. A. Gourley and N. F. Britton, J. Math. Biol. **34**, 297 (1996).

[2] Y. E. Maruvka and N. M. Shnerb, Phys. Rev. E **73**, 011903 (2006).

[3] A. Sasaki, J. Theor. Biol. **186**, 415 (1997).

[4] M. A. Fuentes, M. N. Kuperman and V. M. Kenkre, Phys. Rev. Lett. **91**, 158104 (2003).

[5] M.A. Fuentes, M.N. Kuperman and V.M. Kenkre, J. Phys. Chem. B **108**, 10505 (2004).

[6] E. Hernandez-Garcia and C. Lopez, Phys. Rev. E **70**, 016216 (2004).

[7] G. Flierl, D. Grunbaum, S. Levin and D. Olson, J. Theor. Biol. **196**, 397 (1999).

[8] B. M. Bolker, Theor. Popul. Biol. **64**, 255 (2003).

[9] J. Roughgarden, Am. Nat. **106**, 683 (1972); F. Bagnoli and M. Bezzi, Phys. Rev. Lett. **79** 3302 (1997); U. Dieckmann and M. Doebeli, Nature **400**, 354 (1999); M. Doebeli and U. Dieckmann, Nature **421**, 259 (2003); E. Brigatti, J. S. Sá Martins and I. Roditi, Physica A **376**, 378 (2007); V. Schwämmle and E. Brigatti, Europhys. Lett. **75**, 342 (2006).

[10] W. R. Young, A. J. Roberts and G. Stuhne, Nature **412**, 328 (2001).

[11] R. A. Fisher, Ann. Eugenics **7**, 353 (1937); A. Kolmogoroff, I. Petrovsky and N. Piscounoff, Moscow Univ. Bull. Math. **1**, 1 (1937).

[12] J. Polechova and N. H. Barton, Evolution, **59**, 1194 (2005).

[13] Y.-C. Zhang, M. Serva and M. Polikarpov, J. Stat. Phys. **58**, 849 (1990); M. Meyer, S. Havlin and A. Bunde, Phys. Rev. E **54**, 5567 (1996); N. M. Shnerb, Y. Louzoun, E. Bettelheim and S. Solomon, Proc. Natl. Acad. Sci. U.S.A. **97**, 10322 (2000); B. Houchmandzadeh, Phys. Rev. E **66**, 052902 (2002).

[14] C. Lopez and E. Hernandez-Garcia, Physica D **199**, 223 (2004).

[15] E. Hernandez-Garcia and C. Lopez, Physica A **356**, 95 (2005).

[16] E. Hernandez-Garcia and C. Lopez, J. Phys.: Condens. Matter **17**, S4263 (2005).
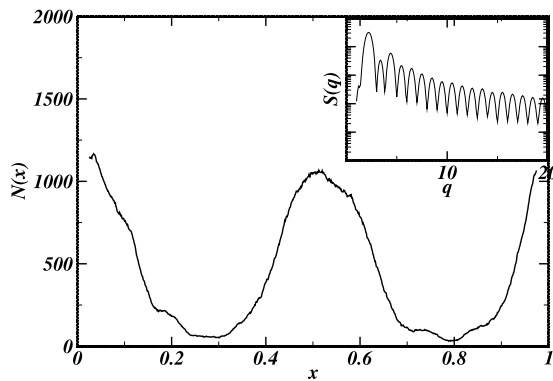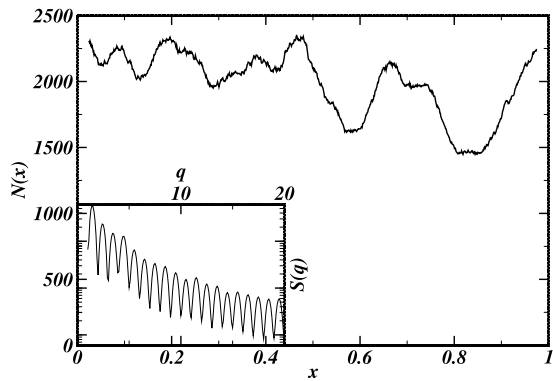
FIG. 1. Homogeneous steady state distribution (on the top, $C = 4.0, 1/K = 80000, \sigma = 0.01$) and modulated steady state distribution (on the top, $C = 0.9, 1/K = 18000, \sigma = 0.01$). The insets show the structure functions, $S(q)$, of the corresponding simulations. We show the distributions at time step 1000, whereas the structure functions are averaged over 500 time steps.
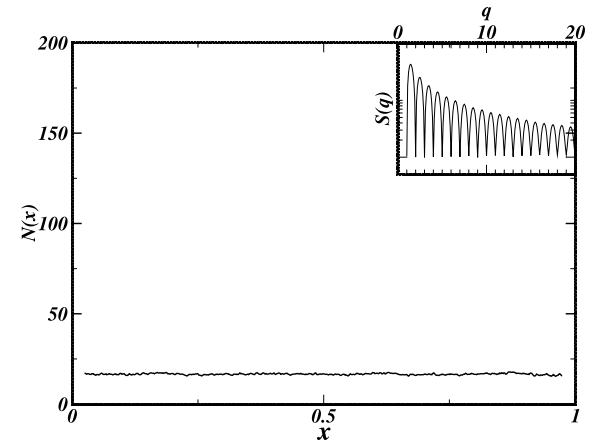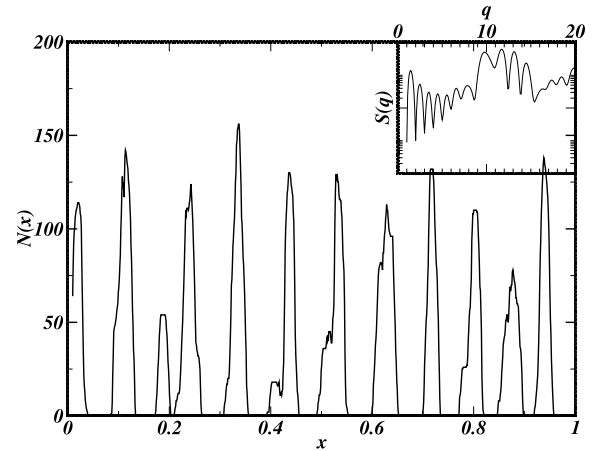

FIG. 2. Spiky steady state (on the left, $C = 0.059$, $1/K = 500$, $\sigma = 0.001$) and homogeneous steady state (on the right, $C = 0.005$, $1/K = 500$, $\sigma = 0.001$). The insets show the structure functions $S(q)$. We show the distributions at time step 2000, whereas the structure functions are averaged over 1000 time steps. The transition between these two states, in this typical range of parameters, has been extensively studied.
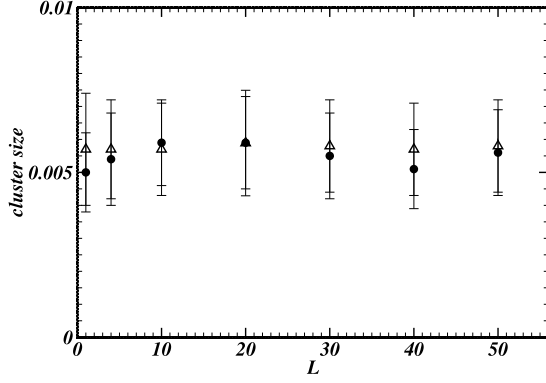
FIG. 3. Dependence of the cluster size on the ring size L. We present data from the model with mutation (triangles) and from the one that implements diffusion (circles), $C = 0.2, K = 0.0029, \sigma = 0.001$. The average is carried out over all the clusters present at a given time step and over different time steps.
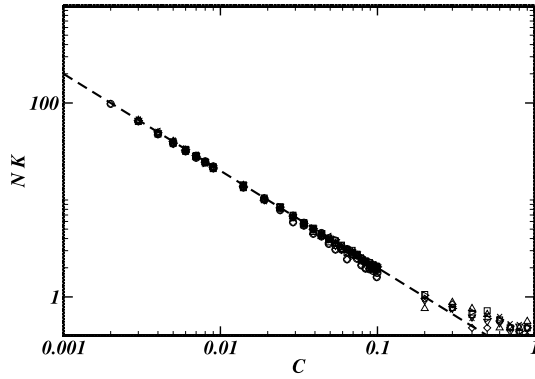

FIG. 4. The number of individuals N present in the steady state is proportional to $(CK)^{-1}$. This result is in accordance with the one obtained for a box-type influence function of length C (see ref. [14]). We present data for different simulations with $1/K \in [50, 500]$ and $\sigma \in [0.0001, 0.01]$. This last parameter does not influence the final number of individuals. The dashed line has slope -1.
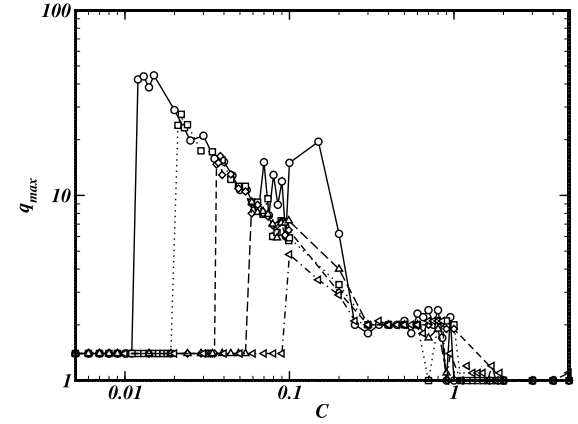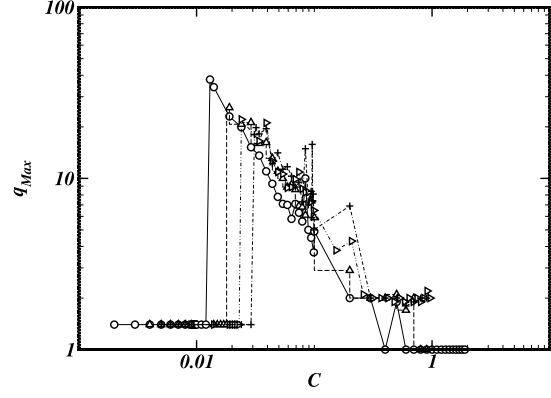
FIG. 5. Segregation transition at $C_{critical}$. Upper figure: variation in dependence of K. From left to right: $1/K = 50, 150, 400, 500$; $\sigma = 0.001$. Lower figure: variation in dependence of σ. From left to right: $\sigma = 0.0005, 0.001, 0.002, 0.005, 0.01$; $1/K = 200$.
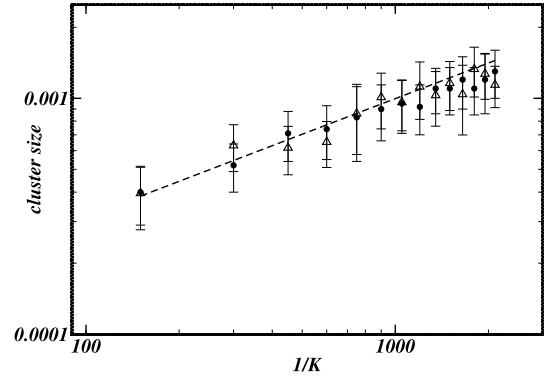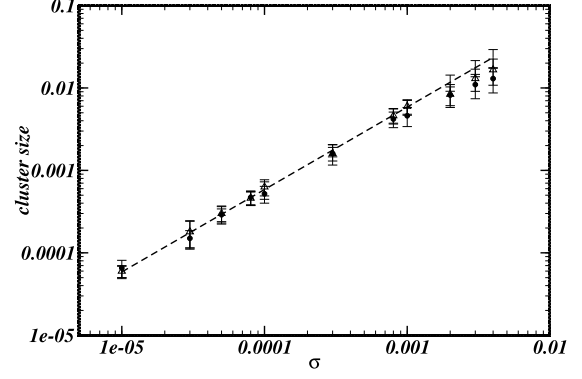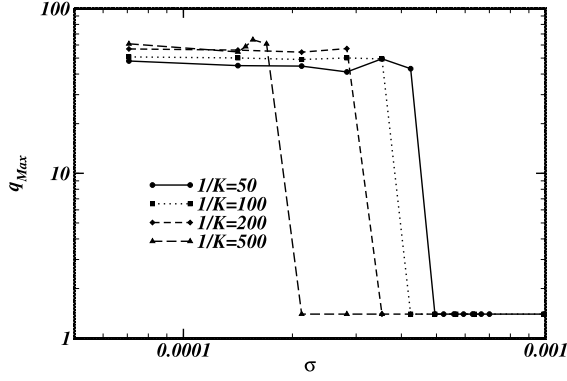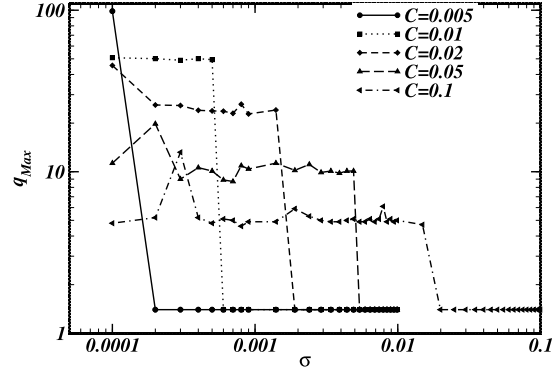
FIG. 7. On the top, cluster size as a function of σ; $1/K = 300$. The solid line has slope 1. On the bottom, the cluster size as a function of $1/K$; $\sigma = 0.0001$. The solid line has slope $1/2$. Triangles represent data from the simulations where diffusion is implemented through mutations, circles for the direct implementation of the diffusive process; we set $C = 0.09$.

FIG. 6. As shown in these figures, a critical σ value exists, above which no spatial structures emerge. Upper figure: variation in dependence of C; we set $1/K = 100$. Lower figure: variation in dependence of K; we set $C = 0.01$.
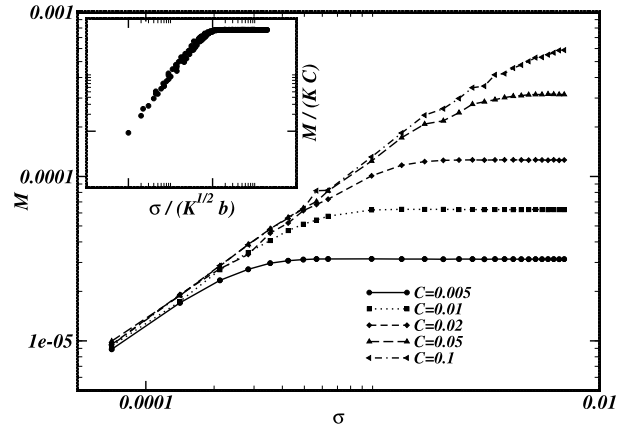
FIG. 8. Mobility dependence on the diffusion parameter σ for different C values; $K = 0.01$. In the inset, the data collapse for arbitrary values of the parameters.
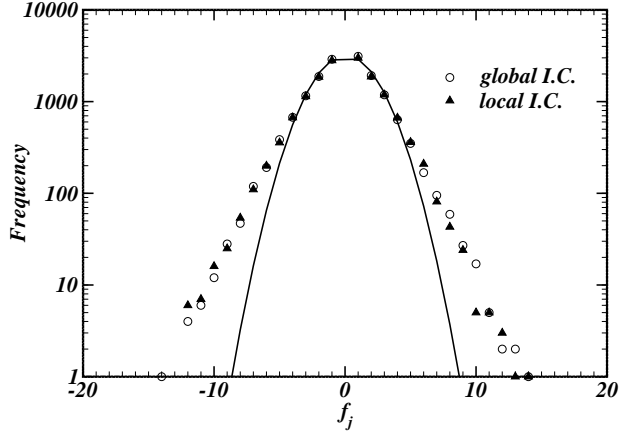
FIG. 9. Spatial local fluctuation distribution at the steady state: deviation from a Gaussian ($C = 0.1$, $K = 0.00005$, $\sigma = 0.0017$). Data are averaged over 5 time steps. The continuous line is the best fitted Gaussian.